ISSN 0208-7774 TRIBOLOGIA 5/2018 p. 5–12

Paweł BAGIŃSKI*, Grzegorz ŻYWICA*

EXPERIMENTAL INVESTIGATION OF A FOIL BEARING STRUCTURE WITH A POLYMER COATING UNDER DYNAMIC LOADS

BADANIA EKSPERYMENTALNE STRUKTURALNEJ WARSTWY NOŚNEJ ŁOŻYSKA FOLIOWEGO Z POWŁOKĄ POLIMEROWĄ W ZAKRESIE OBCIĄŻEŃ DYNAMICZNYCH

Key words: gas foil bearings, high-speed bearings, dynamic load, dynamic stiffness.

Abstract This paper presents the results of research on the structural elements of a prototypical foil bearing in terms of its dynamic loads. In the framework of dynamic tests, several dozens of measurement series were carried out on a test rig specially prepared for this purpose. Dynamic excitations were applied using an electromagnetic exciter that enables changing the amplitude and frequency of the excitation force. Owing to this, it was possible to determine characteristics of the tested system in a wide range of loads and frequencies. A value of 400 Hz was assumed as the upper limit of the excitation frequency. The test rig enabled considering the direction of dynamic loads, which, as it turned out, had a significant impact on the obtained results. The research findings show that both the amplitude and frequency of an excitation force have a major impact on the stiffness and damping of the structural part of the foil bearing. The results of dynamic load tests complement the results of static tests performed earlier.

Słowa kluczowe: gazowe łożyska foliowe, łożyska wysokoobrotowe, obciążenie dynamiczne, sztywność dynamiczna.

Streszczenie Przedstawiono wyniki badań elementów strukturalnych prototypowego łożyska foliowego w zakresie obciążeń dynamicznych. W ramach badań dynamicznych przeprowadzono kilkadziesiąt serii pomiarowych na specjalnie do tego celu przygotowanym stanowisku badawczym. Wymuszenie dynamiczne było realizowane za pomocą wzbudnika elektromagnetycznego, umożliwiającego zmianę amplitudy i częstotliwości siły wymuszającej. Pozwoliło to na wyznaczenie charakterystyk badanego układu w szerokim zakresie obciążeń i częstotliwości. Jako górną granicę częstotliwości wymuszenia przyjęto 400 Hz. Zastosowane stanowisko laboratoryjne pozwoliło na uwzględnienie różnych kierunków działania obciążenia dynamicznego, co, jak się okazało, miało istotny wpływ na uzyskiwane wyniki. Przeprowadzone badania wykazały, że zarówno amplituda, jak i częstotliwość wymuszenia mają bardzo duży wpływ na sztywność i tłumienie strukturalnej części łożyska foliowego. Wyniki badań w zakresie obciążeń dynamicznych stanowią uzupełnienie wcześniej przeprowadzonych testów statycznych.

INTRODUCTION

Foil bearings are slide bearings in which additional elements (of high compliance and good vibration-damping properties) are placed between the journal and the bush. Gas foil bearings (GFBs) enable the operation of turbomachines at very high speeds and at high temperatures. The above-mentioned elastic-damping elements, which usually have the form of appropriately shaped thin metal foils, are the key elements of foil bearings. These elements can have a big impact on the static and dynamic properties of a foil bearing and enable active shaping of its characteristics [**L. 1, 2**]. There are two methods for determining bearing properties, namely, using a numerical model or experimental research, or both. Numerical analyses are very difficult to conduct,

* The Szewalski Institute of Fluid-Flow Machinery of the Polish Academy of Sciences in Gdańsk, Department of Turbine Dynamics and Diagnostics, ul. Fiszera 14, 80-231 Gdańsk, Poland, e-mail: gzywica@imp.gda.pl, pbaginski@imp.gda.pl.

because the gaseous lubricating film and the top foil (which is elastic and can change its shape on being pressed) interact with one another in a GFB. In addition, complex contact phenomena (including friction) [**L. 3**], whose theoretical description is very difficult, take place in the operating bearing. Currently, numerical models are sufficiently reliable that they can be used to design a foil bearing, but the foils themselves cannot be produced in large quantities on a repetitive basis. As a matter of fact, each manufactured bearing may vary in stiffness and/or damping coefficients. Therefore, GFBs are usually subjected to experimental research [**L. 4, 7**] (which allow improving numerical models) before they are used in high-speed machinery. As already mentioned above, the stiffness and damping of the foil assembly are important parameters determining the dynamic properties of each and every rotor supported by GFBs. An identification of these properties is usually done using a test rig that consists of the following elements: a shaft supported on one of its ends by the test bearing, a vibration exciter, and displacement sensors [**L. 8**]. The dependence of stiffness/damping on the excitation frequency is determined, which allows one to identify properties of the bearing (e.g., its energy dissipation ability) [**L. 9**].

This article discusses the research carried out on a newly designed and manufactured GFB. The bearing's top foil is coated with a friction reducing material, which could have affected the obtained results. The parameters that describe the properties of foil bearings, which are known to be strongly non-linear, can be determined during their operation [**L. 10**]. Obtained results of experimental tests will be used to verify numerical models that, in turn, will help in the optimisation of the foil bearing's design.

CHARACTERISTICS OF THE TEST RIG AND THE TEST OBJECT

The research of dynamic characteristics of the load-carrying layer of a new foil bearing was carried out on the test rig designed especially for this purpose (**Fig. 1**). The GFB was located on the shaft (with a diameter of 34 mm), which was mounted on very rigid supports that prevented its deflection. Displacements of the journal were controlled using displacement sensors to check if there was any clearance between the shaft and the supports. The bearing was placed inside a sleeve with notches (spaced 15 degrees from each other, see **Fig. 2**), similarly as shown in article [**L. 11**]. The sleeve has two threaded holes. In one of them, a force sensor was mounted. In the other hole, a screw was placed that blocked the movement of the sleeve in relation to the bearing bush. The vibration exciter was fixed to a rigid structure that was built using aluminium profiles. It was connected via the force sensor and stringer (made of plastic) to the sleeve inside which the bearing was placed. Displacements were measured in two directions using high precision laser sensors. The photo presented

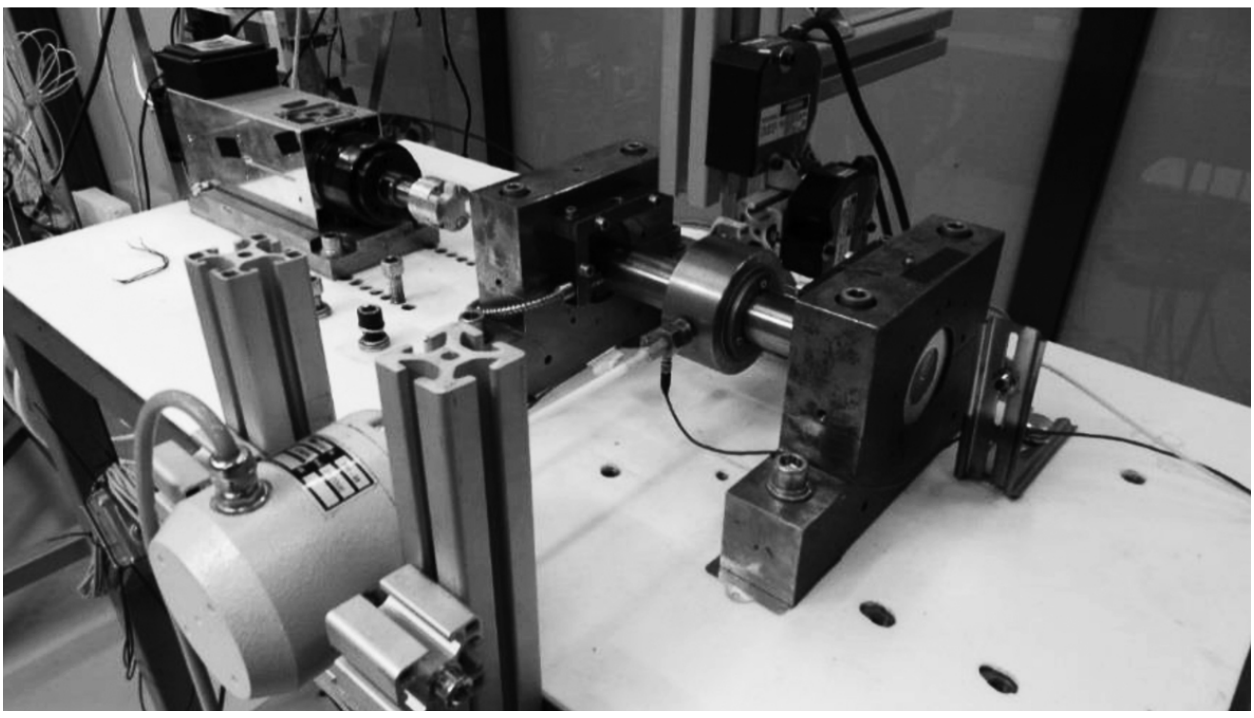

Fig. 1. Test rig on which the structural supporting layer of a foil bearing was tested
Rys. 1. Stanowisko do badania strukturalnej warstwy nośnej łożyska foliowego

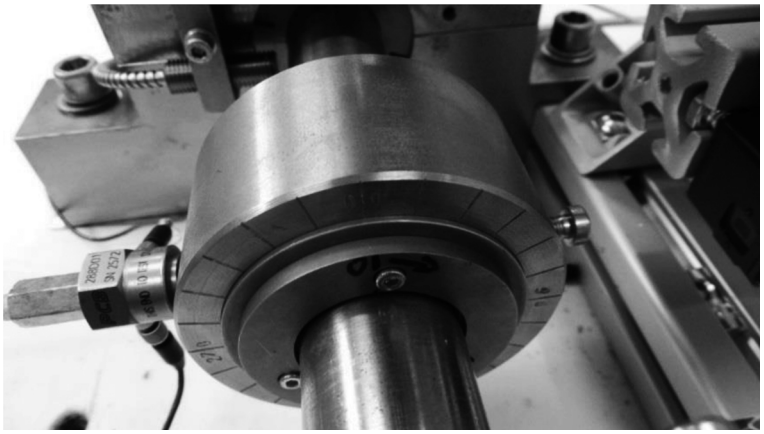

Fig. 2. Tested bearing with the sleeve and force sensor
Rys. 2. Badane łożysko wraz z tuleją i czujnikiem siły

in **Fig. 1** also shows other elements that were not used in the research discussed herein. These are subassemblies that had been used on the same test rig during such tests as endurance tests and rotor dynamics tests [**L. 12**].

A diagram of the test system is presented in **Fig. 3**. On the left-hand side of this figure, a diagram of the test rig is shown. On the right-hand side is a diagram of the tested GFB with marked positions of the bearing bushing and the direction of its rotation. The applied stringer has a high stiffness in the direction of vibration excitation, which guaranteed the transfer of generated forces from the vibration exciter to the foil bearing's bush. In the direction perpendicular to the axis of the stringer, its stiffness is lower, which minimised the influence of an excitation whose direction is not perpendicular to the bushing axis.

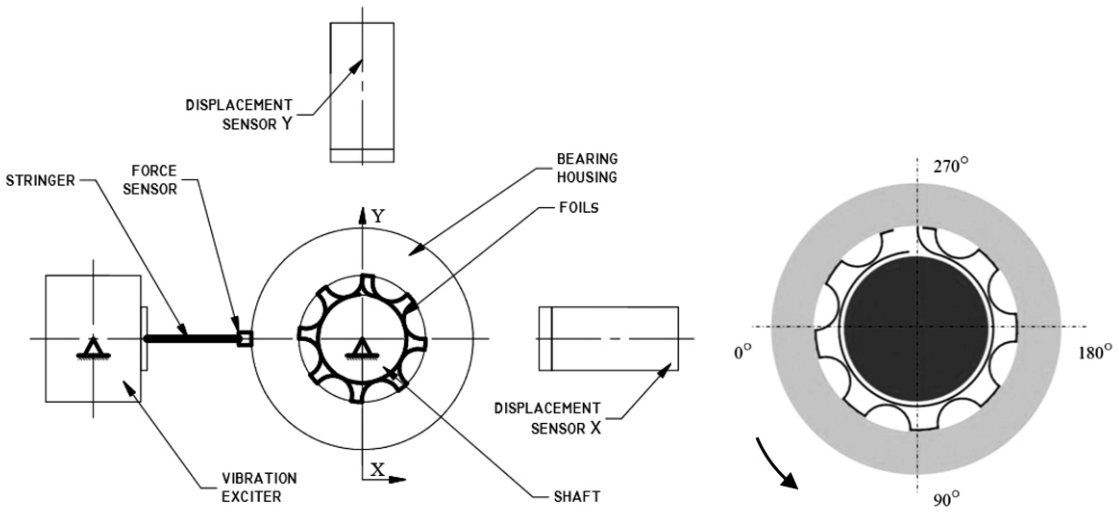

Fig. 3. Diagram of the test rig on which are marked basic components
Rys. 3. Schemat stanowiska badawczego z opisem podstawowych elementów

All sensors and a signal amplifier were connected to a SIEMENS LMS SCADAS control and acquisition system. The results of experimental research are shown in the form of vibration trajectories of the bushing for chosen excitation frequencies and hysteresis loops, where displacements are presented as functions of the excitation force.

The research was performed on a prototypical foil bearing. The new bearing (with a diameter of 34 mm and a length of 40 mm) consists of three sections of the bump foil, one top foil, and the housing. The top foil was coated on one side with a thin polymer layer in order to reduce friction during run-up/run-down of the rotor. Each section

of the bump foil has circumferential notches. All foils have a thickness of approx. 100 μm. Geometrical dimensions of the bump foil are presented in **Fig. 4**. Even though the bearing has a hole in which a thermocouple could have been placed, no temperature measurements were made.

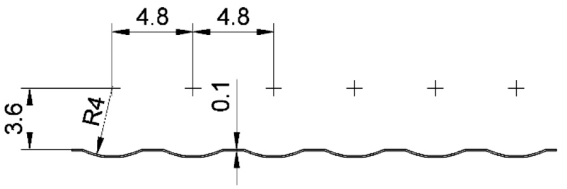

Fig. 4. Geometrical dimensions of the bump foil
Rys. 4. Wymiary geometryczne folii falistej

RESULTS OF EXPERIMENTAL TESTS

During the tests, both the frequency and magnitude of the excitation force were altered. The dynamic force was generated by an electromagnetic vibration exciter. Its direction was constant throughout the tests but its sense changed at a certain frequency. In each measurement series, displacements of the bearing bushing as a function of the excitation force were registered for various excitation frequencies. Each measurement took 10 seconds, during which the force was increased from 5 N to approximately 60 N. Hysteresis loops and vibration trajectories of the bushing are shown for the maximal force at a given frequency. The measurements were carried out for four positions of the bushing, starting from the position at which the lock that fastens the top foil was placed on top, and then the bushing was rotated by 90° in the opposite direction to the direction of the journal's revolutions (**Fig. 3**). The tables below show the displacement curves that were registered by displacement sensors (black lines) as well as their corresponding loops plotted with red lines using the band-pass filter in the range of ±1 Hz (for a given frequency). An excitation force generated by the vibration exciter, acting in a given direction, changed its sense for the tested position of the bearing, so turning the vibration exciter by 180° should result in obtaining the identical displacement curve. In the article, displacements versus excitation forces were shown only for selected frequencies and only for two positions of the GFB. The first and third columns of the tables contain hysteresis loops (displacement of the bearing versus excitation forces), while the second and fourth columns contain vibration trajectories of the bearing during the tests at given frequencies. Upper graphs correspond to the angular position of 0° in which there was no lock on the top foil on the direction of the excitation. Lower graphs show the results obtained after turning the bearing by 270° (**Fig. 3**).

Table 1 shows hysteresis loops obtained after applying the dynamic excitation with a frequency of 1 Hz to the bearing that was at an angular position of 0° and 270° as well as the vibration trajectories of the sleeve registered during this test. Although the magnitude of the excitation force was similar for both angular positions, the GFB's displacements differ. In both tests, hysteresis loops are large, indicating that, despite the friction between components of the bearing, it exhibited good vibration-damping properties [**L. 13**]. Certain fragments of the curves have irregular shapes,

Table 1. Hysteresis loops and vibration trajectories for two positions of the bush, at the excitations with a frequency of 1 Hz and 20 Hz
Tabela 1. Pętle histerezy oraz trajektorie drgań dla dwóch pozycji panwi przy wymuszeniu o częstotliwości 1 Hz i 20 Hz

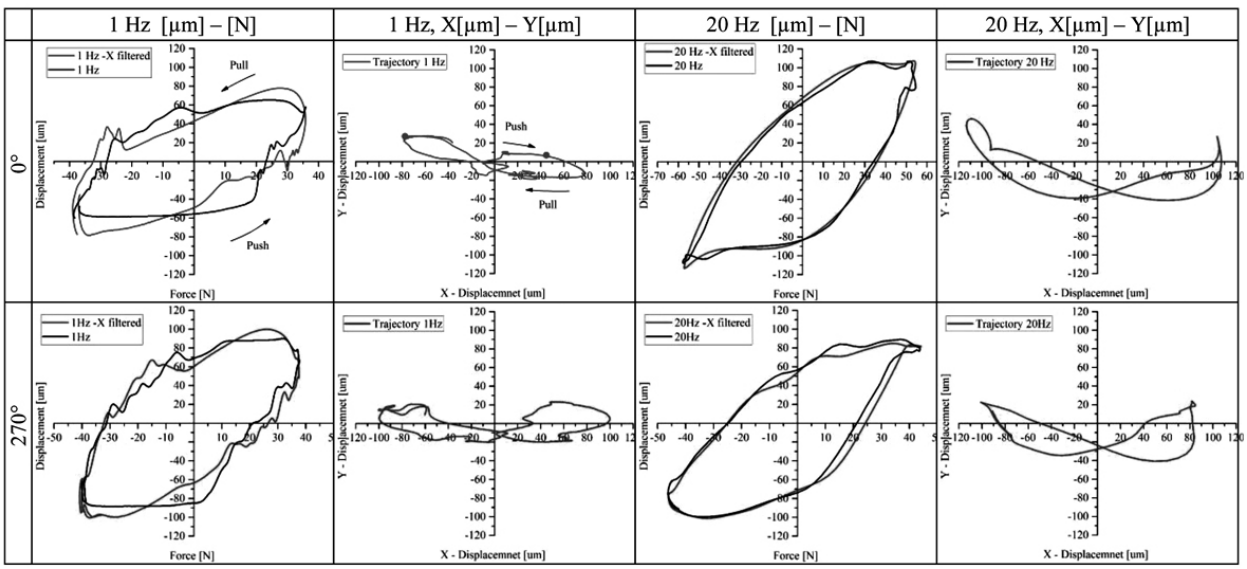

which indicate that the bump foil changed its position or shape, or both. After that change, the shape of the curves became regular, which means that the stiffness of the assembly of foils had increased. The bearing exhibited higher stiffness at an angular position of 0° than at the other angular positions. Moreover, the displacement of the sleeve was lower by 20 μm, and the bearing had worse vibration-damping properties when the excitation with a frequency of 1 Hz was applied to it. This was due to a very short distance (20 μm) between the lock of the foils and the point at which excitation forces were applied. It is also interesting to note that displacements of the tested GFB are not only in the direction in which the force acts but also in the direction perpendicular to this direction. The points at which the forces were maximal and minimal are marked using red dots. On the graphs showing hysteresis loops, arrows were placed to indicate the direction in which the excitation force acted (in other words, to indicate when the vibration exciter was pushing or pulling the bearing). Such arrows could be placed on other graphs.

Table 1 also shows hysteresis loops and vibration trajectories of the GFB for the dynamic excitation with a frequency of 20 Hz. At this excitation frequency, the displacement of the bearing bushing in the X direction was higher (by approx. 20 μm) for an angular position of 0° than for an angular position of 270°. For an angular position of 0°, a higher magnitude of the force (60 N) was obtained at a displacement of approximately 120 μm. For the other angular position, a maximum force of 45 N occurred during pulling the sleeve and the vibration trajectory is flattened (the assembly of foils had higher stiffness), which was caused by the rigid fixing of the foil using the lock. At this maximum force, the bearing had poor vibration-damping properties. But when the excitation acted in the opposite direction, the assembly of foils exhibited good vibration-damping properties. Both hysteresis loops are similar to hysteresis loops shown by other researchers in publication [**L. 13**]. However, they did not present any vibration trajectories of the bushing. Up to an excitation frequency of about 50 Hz, the structural supporting layer of the GFB exhibited varying stiffness values in both directions, so vibration trajectories are not elliptical in shape.

At an excitation frequency of around 80 Hz, hysteresis loops are circular for both positions of the GFB, because the bearing oscillates at a frequency close to its resonant frequency. At the maximum force, the displacement was 0 μm, and, at a force equal to 0 N, it reached the maximum value. This means that there was a phase shift between the excitation force and the dynamic response of the system. When the excitation frequency was set to 80 Hz, the vibration trajectory of the bushing was flattened and largest displacements occurred in the direction the dynamic force acted. This force reached 50 N at an angular position of 0° resulting in a displacement of 100 μm, which indicates a high stiffness of the bearing as well as good vibration-damping properties. At the second angular position of the GFB, the maximum excitation force was lower by 10 N, but the displacement was higher by 20 μm. Even though the stiffness of the bearing was lower than in the previous case, its vibration-damping capability was still good. The results obtained for both angular positions differ significantly.

Table 2. Hysteresis loops and vibration trajectories for two positions of the bush, at the excitations with a frequency of 80 Hz and 110 Hz

Tabela 2. Pętle histerezy oraz trajektorie drgań dla dwóch pozycji panwi przy wymuszeniu o częstotliwości 80 Hz i 110 Hz

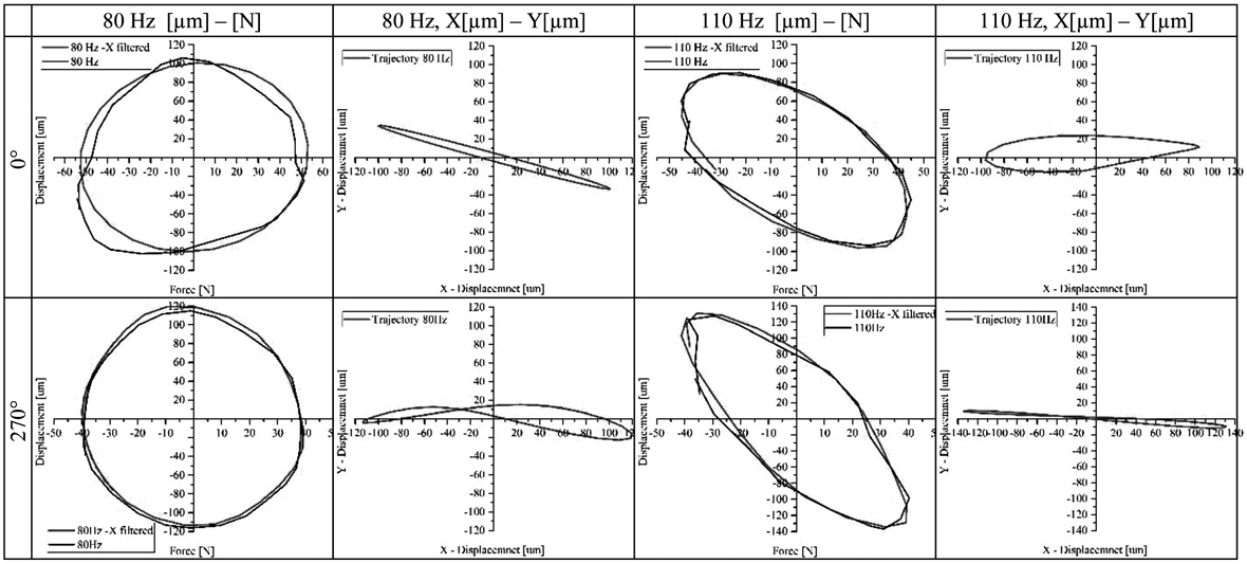

At the dynamic excitation with a frequency of 110 Hz, the shape of the hysteresis loop has changed. The bearing bushing vibrated in counter-phase to the excitation force. When the bushing was set to an angular position of 270°, the displacement of the bearing bushing achieved a value of 140 μm at a force of 40 N, which means that the stiffness of the bearing decreased and thus its vibration-damping ability deteriorated (the hysteresis loop is smaller as shown in **Table 2**). For an angular position of 0°, the obtained force was higher, but the displacements were lower, and the vibration damping was improved. The vibration trajectory of the bushing is flattened, which clearly indicates that the bearing vibrated in one direction under the dynamic force.

Table 3 presents hysteresis loops for the dynamic excitation with a frequency of 200 Hz. They are flattened. The stiffness of the structural supporting layer of the bearing increased, because, even at a force of about 40 N, the displacement of the bushing was only 10 μm (for both angular positions). Furthermore, the hysteresis loops decreased in size, which indicates that the bearing had much worse vibration-damping capability than in the previous cases. Moreover, the hysteresis loop obtained for the second angular position is not a closed curve, which means that the bearing parameters are not constant on both its sides. The vibration trajectories of the bushing are very small and elliptical in shape.

For the excitation force with a frequency of 400 Hz, the bearing had virtually no vibration-damping capability; the foil assembly was very rigid and even a force with a magnitude of approx. 50 N did not cause its deflection.

Table 3. Hysteresis loops and vibration trajectories for two positions of the bush, at the excitations with a frequency of 200 Hz and 400 Hz

Tabela 3. Pętle histerezy oraz trajektorie drgań dla dwóch pozycji panwi przy wymuszeniu o częstotliwości 200 Hz i 400 Hz

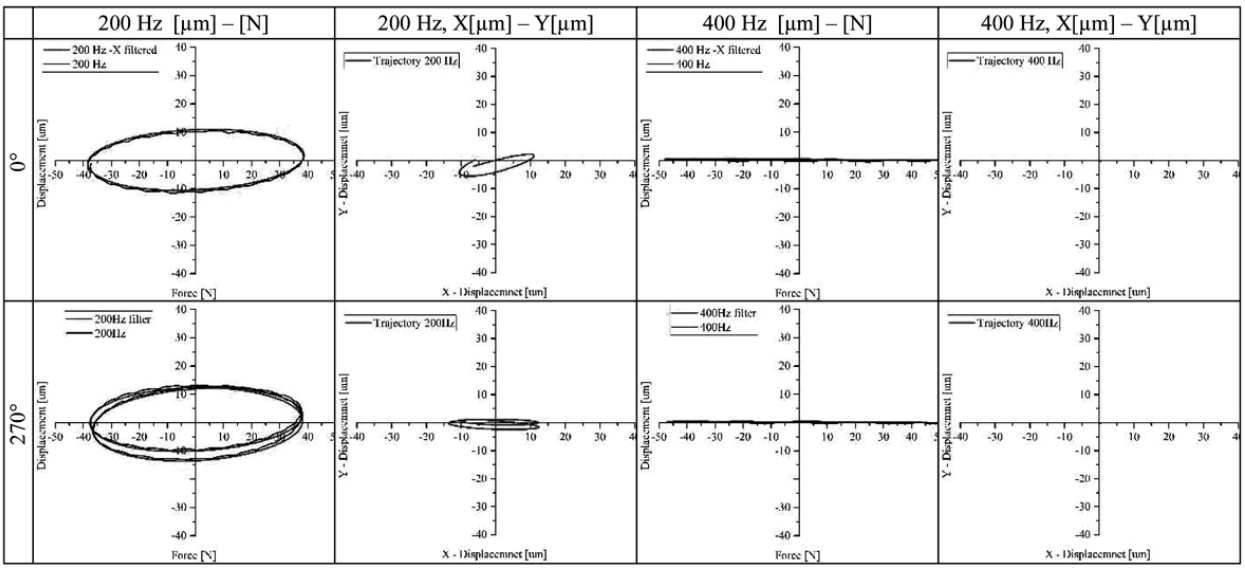

CONCLUSIONS

The article discusses results of the research carried out on a newly engineered foil bearing that was subjected to dynamic loads. The top foil of this bearing was coated with a polymer. The research results were presented using graphs that show the relationships between excitation forces and displacements. The obtained hysteresis loops indicate that the foil assembly is able to efficiently dissipate vibrational energy. Moreover, vibration trajectories of the bearing bush, on which excitation forces with various frequencies were acting, are presented.

Only the results concerning the range of excitation frequencies at which the GFB had the best dynamic performance are shown in the article. Throughout this whole range, such parameters as stiffness and the damping of the foil assembly were changing. When the excitation forces had low frequencies, the bearing exhibited a very good ability to dissipate vibrational energy. It may be said that the bearing has a progressive structure, since, the higher the excitation force, the lower are the displacements of the bush. At some frequencies, hysteresis loops were significantly smaller in size, which means that the GFB quickly reacted to a change in the direction the excitation force acted. The non-linear stiffening of the foil assembly is caused by greater participation of consecutive bumps of the bump foil in supporting the journal.

In the frequency range of 80 Hz to 100 Hz, the bearing's operation changed. The stiffness of the foil assembly remained at the same level, but the bearing damped the vibration more. The GFB vibrated in counter-phase to the excitation force. For higher excitation frequencies (up to 200 Hz), the foil bearing was still able to successfully damp vibration, in spite of the fact that the stiffness of its structure increased as the frequency increased. This frequency seems to be optimal in terms of the dynamic performance of the bearing. After an increase of the frequency of the excitation force, the foil assembly became very rigid, and the force of the same magnitude that earlier had been able to cause a deflection of the foil assembly was no longer able to do so.

In addition, a vibration trajectory of the bushing was placed next to each hysteresis loop. The test rig was built using information obtained from other scientific publications (the titles of which are given in the references). It is important to note that other researchers have not observed during their experiment that the bushing vibrated in a direction that was perpendicular to the direction the excitation force acted. The obtained trajectories show that, when the stiffness of the bearing assembly increased under the dynamic force, the bearing bushing vibrated in the direction in which the bearing's stiffness was lower, i.e. in the direction that was perpendicular to the direction in which the excitation force acted.

The obtained results will be used to verify the numerical model of the newly engineered foil bearing. Furthermore, such a model could be used to optimise the geometric dimensions of the bearing's structure in order to obtain better dynamic performance in a wider frequency range. It will then be possible to use these enhanced foil bearings in high-speed machines of different types (e.g., in microturbines).

ACKNOWLEDGEMENT

The research was carried out under project No. 2016/21/D/ST8/01711, financed by the National Centre of Science (NCN).

REFERENCES

1. Andrés L.S. and Kim T.H.: Forced nonlinear response of gas foil bearing supported rotors, Tribol. Int., Aug. 2008, vol. 41, no. 8, pp. 704–715.
2. Tabares D.R.: Rotordynamic Performance of a Rotor Supported on Bump-type Foil Bearings: Experiments and Predictions, J. Chem. Inf. Model., 2013, vol. 53, no. 9, pp. 1689–1699.
3. San Andrés L., Norsworthy J.: Structural and Rotordynamic Force Coefficients of a Shimmed Bump Foil Bearing: An Assessment of a Simple Engineering Practice, J. Eng. Gas Turbines Power, 2016, vol. 138, no. 1, p. 12505.
4. Dykas B., Bruckner R., DellaCorte C., Edmonds B., Prahl J.: Design, Fabrication, and Performance of Foil Gas Thrust Bearings for Microturbomachinery Applications, J. Eng. Gas Turbines Power, 2009, vol. 131, no. 1, p. 12301.
5. Łagodziński J., Miazga K. and Musiał I.: Application of a compliant foil bearing for the thrust force estimation in the single stage radial blower, Open Eng., 2015, vol. 5, no. 1.
6. Emerson T.P.: The Application of Foil Air Bearing Turbomachinery in Aircraft Environmental Control Systems, in ASME Intersociety Conference on Environmental Systems, pp. 780-NaN-18.
7. Hou Y., Yang S., Chen X., Chen R., Lai T., Chen S.: Application of compliant foil bearings in a cryogenic turboexpander, Harbin Gongcheng Daxue Xuebao/Journal Harbin Eng. Univ., 2015, vol. 36, no. 4.
8. San Andrés L., Ryu K. and Kim T.H.: Identification of Structural Stiffness and Energy Dissipation Parameters in a Second Generation Foil Bearing: Effect of Shaft Temperature, J. Eng. Gas Turbines Power, 2011, vol. 133, no. March, p. 32501.
9. Feng K., Hu J., Liu W., Zhao X., Li W.: Structural Characterization of a Novel Gas Foil Bearing With Nested Compression Springs: Analytical Modeling and Experimental Measurement, J. Eng. Gas Turbines Power, 2016, vol. 138, no. 1, p. 12504.
10. DellaCorte C., Radil K.C., Bruckner R.J., Howard S.A.: Design, Fabrication, and Performance of Open Source Generation I and II Compliant Hydrodynamic Gas Foil Bearings, Tribol. Trans., 2008, vol. 51, no. 3, pp. 254–264.
11. Rubio D., San Andrés L.: Bump-Type Foil Bearing Structural Stiffness: Experiments and Predictions," J. Eng. Gas Turbines Power, 2006, vol. 128, no. 3, p. 653.

12. Zywica G., Baginski P., Banaszek S.: Experimental Studies on Foil Bearing with a Sliding Coating Made of Synthetic Material, J. Tribol., 2016, vol. 138, no. 1.
13. Feng K., Liu Y., Zhao X., Liu W.: Experimental Evaluation of the Structure Characterization of a Novel Hybrid Bump-Metal Mesh Foil Bearing, J. Tribol., 2015, vol. 138, no. 1, p. 21702.